Influence of Grafting Density and Distribution on Material Properties Using Well-Defined Alkyl Functional Poly(Styrene-*co*-Maleic Anhydride) Architectures Synthesized by RAFT

Guillaume Moriceau,[a] Joji Tanaka,[a] Daniel Lester,[a] George S. Pappas,[b] Alexander B. Cook, [a] Paul O'Hora,[c] Joby Winn,[c] Timothy Smith,[c] and Sébastien Perrier.[*a,d,e]

[a] Department of Chemistry, The University of Warwick, Coventry CV4 7AL, UK

[b] WMG, The University of Warwick, Coventry CV4 7AL, UK

[c] Lubrizol Limited. The Knowle, Nether Lane, Hazelwood, Derbyshire DE56 4AN, UK

[d] Faculty of Pharmacy and Pharmaceutical Sciences, Monash University, VIC 3052, Australia.

[e] Warwick Medical School, The University of Warwick, Coventry CV4 7AL, UK

TOC use only:

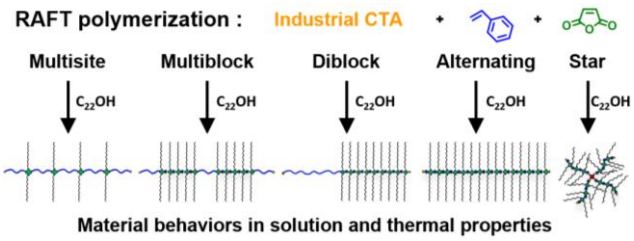

ABSTRACT

Poly(Styrene-*co*-Maleic Anhydride) copolymers (PSMA) with controlled number and distribution of maleic anhydride (MAnh) units were synthesized by reversible addition-fragmentation chain transfer (RAFT) polymerization using chain-transfer agents (CTA) suitable for industrial scale processes. Linear and star shaped alternating PSMA polymers were prepared in a single-step synthesis, while a one-pot sequential chain-extension strategy was utilized to prepare diblock, multiblock and multisite copolymers architectures. A library of grafted PSMAs with controlled density and distribution of side chains was achieved by the subsequent grafting of long aliphatic alcohol chains (C22) to the MAnh units. The influence of structure, composition, and long alkyl chain addition on PSMAs behavior in solution was studied with triple-detection size exclusion chromatography (SEC), while their thermal properties were examined by thermogravimetric analysis (TGA) and differential scanning calorimetry (DSC). Overall, the side chain density and distribution did not impact the polymer conformations in solution (random coil), however, an effect on the molecular size (R_h) and structure density (intrinsic viscosity) were observed. The materials density was shown to be dependent on polymer architectures as lower intrinsic viscosity was observed for star copolymer. All the materials had similar degradation point (400 °C) while, the rate of degradation showed a dependence on the MAnh content and polymeric architecture. Ultimately, the grafting of long aliphatic side chains (crystalline) onto the PSMA backbone,

even at low density, was shown to drastically change the microphase ordering, as all the grafted copolymers became semi-crystalline. The difference of the crystallization temperature between low density multisite materials ($T_c \approx 8$ °C) and the high density alternating material ($T_c \approx 40$ °C), highlights the major importance of controlling copolymer composition and structure to tune material properties.

INTRODUCTION

A significant challenge in modern macromolecular science is to mimic nature to achieve complex copolymers with highly controlled chemical composition and molecular structure.[1, 2] The rise of recent studies on advanced polymeric architectures, such as brushes, star-shaped, cyclic and other functional (co)polymers with controlled grafting density and distribution, suggests an increasing interest in this field.[3-9] Graft copolymers can adopt different conformations (such as coil, rodlike or wormlike) determined by their chemical composition, architecture, and their interaction with the solvent.[10-12] Moreover, the control over grafting density and distribution has also been found to be of fundamental importance when preparing tailored nanoscopic objects with interesting mechanical and physicochemical properties (*e.g.* self-assembling or stimuli-responsive materials).[13-16] Functional copolymers can also offer different properties depending on their grafting density and distribution of functional groups.[17, 18] The control of monomer sequence/distribution itself has been observed to be of interest to control some physical properties of copolymers such as solubility, amphiphilicity, assembly and thermal properties.[19, 20] Recently, the effect of block segregation (multiblock structure) on microphase separation and glass transition temperature (T_g) was demonstrated.[21] Another study on thermo-responsive, spontaneous gradient copolymers showed the effect of monomer sequence and distribution on glass transition and self-assembly behavior.[22] These examples of non-grafted copolymers show the importance of controlling monomer distribution to tune the physicochemical properties of copolymers. Due to the donor-acceptor effect and a high rate

coefficient of cross-propagation (k_{cp}), the radical copolymerization of styrene (Sty) and maleic anhydride (MAnh) is a unique combination that offers sequence controlled copolymers (alternating).[23, 24] Furthermore, the facile functionalization of MAnh moieties offers an efficient way to prepare functional materials of high sequence control, and high density and distribution of the grafted functionalities.[25] Alternating poly(Sty-*alt*-MAnh) (PSMA) materials have been synthesized on an industrial scale by free-radical polymerization since the 1940s, and their derivatives are commonly used in applications such as rheology modifiers, plasticizers, polymeric surfactants and pigment dispersants.[26] Their advantageous mechanical and thermal properties, high chemical resistance and high degree of functionality are regularly described in scientific and technical reviews.[27-29] Moreover, with the recent developments in controlled radical polymerization techniques (CRP) such as metal-mediated radical polymerisation (*e.g.* ATRP and SET-LRP),[30-32] nitroxide-mediated polymerisation[33] and reversible addition-fragmentation chain transfer (RAFT) polymerization,[34, 35] the exceptional features of this donor-acceptor system have been re-investigated to achieve well-defined alternating copolymers (controlled M_n, narrow dispersity),[36-38] polymer end-chain functionalization[39]and single monomer unit insertion.[40-46] PSMA materials with various composition and controlled structure were also synthesized by exploiting the versatility of RAFT polymerization.[47-50]

Recently, our group showed the facile and scalable RAFT synthesis of a PSMA multisite copolymer with MAnh units inserted at precise locations along a polystyrene backbone.[40] The ability to synthesize functional materials with high degree of control on functional group distribution was demonstrated. In a recent study, Srichan *et al.* demonstrated the influence of monomer composition and sequence distribution of octadecyl styrene-*co*-N-substituted maleimide copolymers on the melting and crystallization temperatures of semicrystalline materials, however, this is yet to be investigated for more advanced architectures.[17]

In this work, a library of complex PSMA architectures (alternating, diblock, multiblock,

multisite, and alternating star) was prepared by exploiting a one-pot, sequential chain-extension by RAFT polymerization. Well-defined PSMA materials were produced on gram scale using industrial CTA (technical grade, 80 % pure) (Scheme 1). The PSMA materials were subsequently functionalized with long aliphatic alcohols, leading to graft-like copolymers of controlled side group density and distribution. The grafting density and distribution were evaluated, and their effects on the physical and thermal properties were studied.

Scheme 1. Synthesis of well-defined grafted PSMA copolymers using optimized RAFT polymerization with industrial CTAs and post-polymerization esterification of MAnh units.

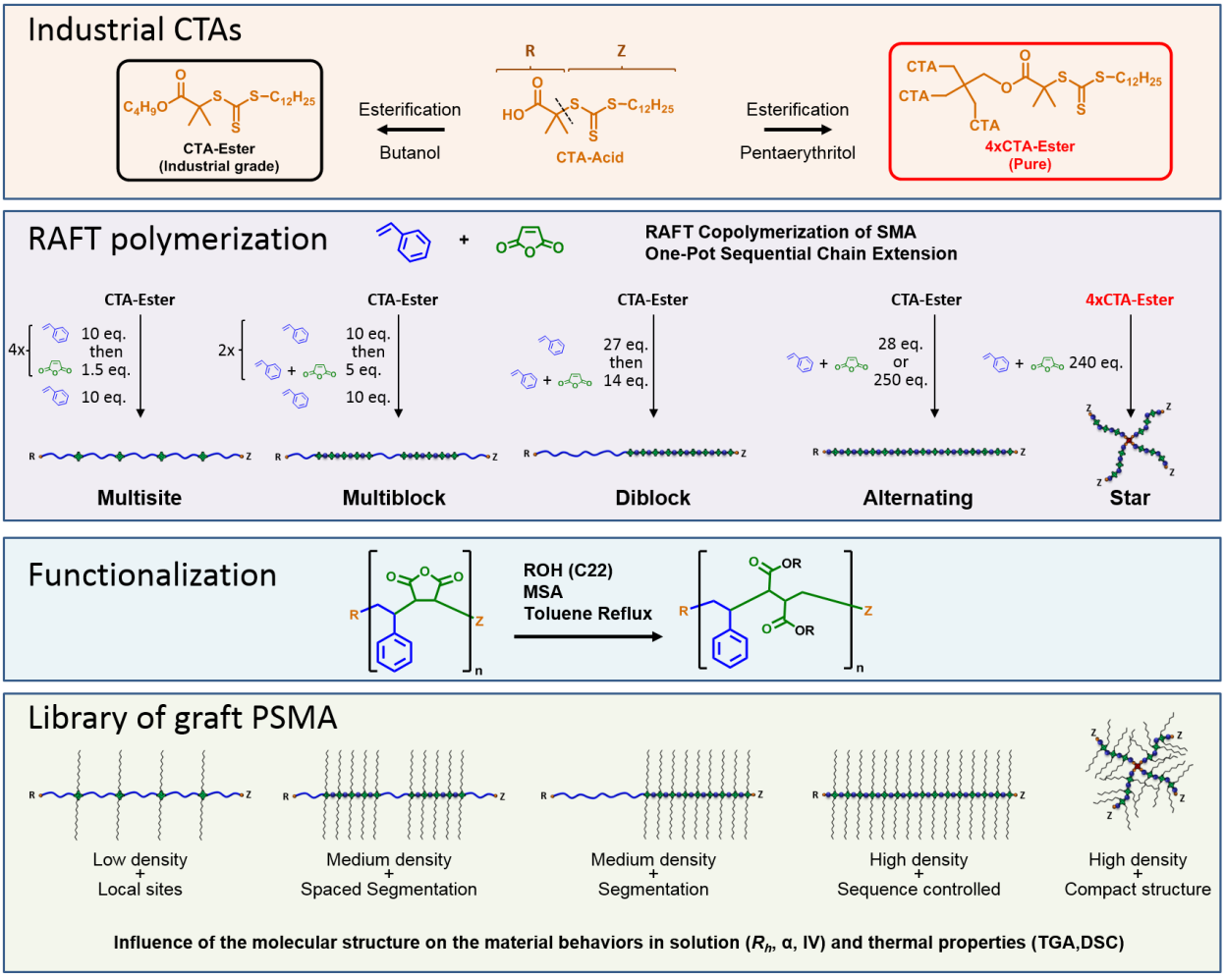

RESULTS AND DISCUSSION

In this work we present the synthesis of well-defined grafted PSMA materials allowing to study the influence of grafting density and distribution on materials' properties (Scheme 1). The PSMA backbones were synthesized by an optimized RAFT polymerization using industrial-grade RAFT agents.[51-53] The rationale behind this is to highlight the feasibility of the method for industrial scale production of polymers with well-defined architecture and composition. The linear copolymers were synthesized using technical grade butyl-2-methyl-2-[(dodecylsulfanylthiocarbonyl)sulfanyl] propionate (CTA-Ester) without purification (80 % pure). The ability to obtain well-defined polymeric architectures from low grade RAFT agents is essential for the development of large scale RAFT process which has been reported in only a few recent studies.[40, 52] Additionally, the synthesis of a tetra-functional CTA-Ester (4xCTA) enabled the preparation of a four arm PSMA star copolymer. The 4xCTA was synthesized following a Dean-Stark process commonly used in industry (Scheme S1) by esterification of CTA-Acid (CTA-Ester precursor) and pentaerythritol in the presence of an acid catalyst (i.e. methane sulfonic acid). Approximately, 1 gram of pure 4xCTA was obtained after purification by column chromatography. The conversion of CTA-Acid into 4xCTA was confirmed by ^{1}H and ^{13}C NMR spectroscopy (Figure S1-S2), and MALDI-ToF-MS (Figure S3).

Four linear PSMA copolymers with comparable molar mass (5,000-6,000 g mol^{-1}) but different monomer unit distributions were synthesized to study the influence of molecular structure on material properties, such as conformation in solution and thermal behavior (Table 1). The maleic anhydride content (density) in each material (total DP ~ 50-56) was varied from 28 units for the alternating (highest density of side chains) to 6 units on average for the multisite copolymer (lowest density). Furthermore, the monomer distribution was tuned from perfectly alternating to a multiblock-like structure, varying the segmentation between the copolymers. A linear alternating PSMA (alt-PSMA-50k) with higher molar mass (50,000 g mol^{-1}), and its star

analogue, were also synthesized to compare the effects of the molar mass and architecture.

Table 1. PSMA Materials Features

Materials		$M_{n,theo}$[a] g mol^{-1}	$M_{n,RI}$[b] g mol^{-1}	$M_{n,3d\text{-}SEC}$[c] g mol^{-1}	$Đ_{RI}$[b]	Nb MAnh [d]
$P[SMA]_{28}$	Alt-Linear	5,600	8,100 [f]	6,200 [f]	1.13 [f]	23
$P[Sty_{27}$-*b*-$(SMA)_{14}]$	Diblock	5,600	5,300 [f]	6,400 [e]	1.22 [f]	13
$P[Sty_{10}$-*b*-$(SMA)_5]_2$-*b*-$PSty_{10}$	Multiblock	5,100	4,100 [e]	5,100 [e]	1.20 [e]	10
$P[(Sty_{10}$-*s*-$MAnh_{1.5})_4$-*b*-$PSty_{10}]$	Multisite	5,900	5,200 [e]	6,400 [e]	1.29 [e]	5
$P[SMA]_{250}$	Alt-Linear	50,700	54,500 [f]	48,200 [f]	1.19 [f]	225
$4xP[SMA]_{60}$	Alt-Star	47,600	47,200 [f]	44,900 [f]	1.15 [f]	200

[a] Calculated by ^{1}H NMR. [b] Obtained using conventional SEC with RI detector. [c] Obtained using triple-detection SEC (3d-SEC). [d] Number of MAnh units calculated from ^{13}C NMR using peak at 172 ppm. [e] SEC in Chloroform. [f] SEC in DMF

Synthesis of alternating PSMA Materials.

The synthesis of alternating PSMA by RAFT is relatively easy to accomplish and was achieved following a methodology adapted from previous studies.[36, 54] The polymerizations were performed at 60 °C using an equimolar feed ratio of Sty and MAnh in the presence of either the industrial grade CTA-Ester or pure 4xCTA. A minimum concentration of initiator (V601; $T_{1/2\text{-}10h}$ = 66 °C) was used to obtain well-defined alternating PSMA materials within 24 hours (conv. > 90 %) (Table S2-S3). Due to the nature of 4xCTA, linked to the core *via* the R group (Scheme 1), the RAFT polymerization occurred *via* core-first strategy and using R group approach.[6, 55] This strategy allows the synthesis of star copolymers with a defined number of arms, growing from the core, however, it is also important to note that this strategy will produce linear species away from the core due to the initiator derived chains and the fragmentation of the Z group. Thus, the star copolymer was synthesized according to previous protocols, where a minimum amount of initiator is added to limit these undesired events.[56] To our knowledge,

this is the first reported example of a 4xPSMA star prepared by RAFT. The formation of well-defined alternating PSMA copolymers was confirmed by ^{1}H NMR spectroscopy (Figure S5-S7), size exclusion chromatography (Figure S8), and MALDI-ToF-MS (Figure S9), all showing good agreement between theoretical and experimental molar mass values and narrow molar mass distribution (Table 1). The alternating nature of the copolymers was confirmed using ^{13}C NMR spectroscopy. Briefly, the local neighboring repeating unit (triad) can be categorically determined by following the relative chemical shift (δ_c) of the quaternary aromatic carbon (C_{arom}) of Sty residue at δ_c =135-150 ppm (Figure 1). It is known that an alternating sequence (M**S**M) shows a main peak at δ_c =135-141.5 ppm while for the random (S**S**M) and homopolystyrene (S**S**S), peaks between δ_c = 141.5-144.5 ppm and δ_c =144.5-148 ppm are observed, respectively.[57, 58] All alternating materials exhibited a main peak between δ_c =135-145 ppm confirming the main alternating nature of their monomer sequences (Figure 1 – D-F). The minor peaks in the random region were attributed to marginal Sty-Sty defects in the microstructures.

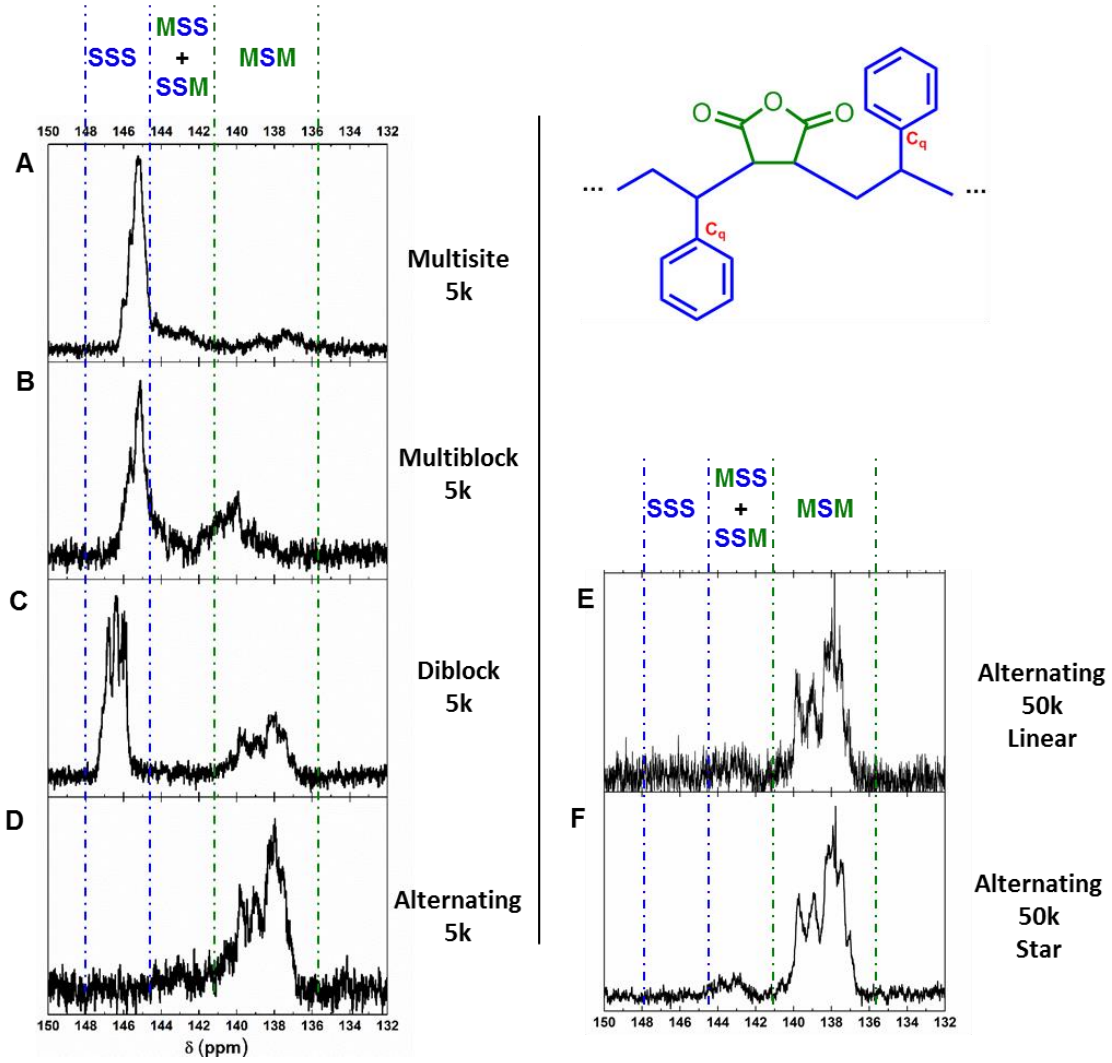

Figure 1. ^{13}C NMR spectra showing quaternary carbon of styrene for materials with different composition.

Synthesis of diblock PSty-*b*-PSMA

The synthesis of block copolymers of PSMA by RAFT in a one-step process (excess of styrene in monomer feed), has been previously described in literature.[49, 50] Although this method is quick and efficient to produce PSMA-*b*-PSty diblocks on large scale, the excess of Sty in the monomer feed increases the probability of defects (Sty-Sty) in the monomer sequence of the PSMA block. Herein, the diblock was synthesized starting with a PSty block of DP = 27 and subsequent chain extension (one-pot) using an equimolar feed of Sty and MAnh to achieve an alternating PSMA block of DP = 14 (Table S4-S5). The first block (PSty macroCTA) was

synthesized with V-40 as initiator ($T_{1/2\text{-}10h}$ = 88 °C) at 100 °C following a procedure developed previously,[40] while the extension step with the SMA block was achieved following the conditions used above for alt-PSMA materials (V601 at 60 °C). Importantly, the complete consumption of V-40 initiator during the first block synthesis allowed the subsequent one-pot chain extension with a different initiator (V601) without taking into account the amount of previous initiator left. The synthesis of a well-defined diblock PSty-*b*-PSMA with molar mass similar to the alternating material and narrow dispersity was confirmed by ^{1}H NMR (Figure S28), SEC (Figure S29-30) and MALDI-ToF-MS (Figure S31). Furthermore, the existence of two distinct peaks in the ^{13}C NMR spectrum (Figure 1 - C) confirmed the presence of blocks with different nature (SSS *vs.* MSM) in the copolymer.

Synthesis of multiblock (PSty-*b*-PSMA)$_2$-*b*-PSty

A multiblock PSMA copolymer was designed to obtain two short blocks of alternating PSMA of DP = 5 separated by PSty blocks of DP = 10 (Table S6-S7). In contrast to the diblock synthesis, a single initiator system (V-40) was used and the concentration of residual initiator after each step was taken into consideration. The PSty blocks were synthesized at 100 °C, however, a lower polymerization temperature of 70 °C was applied for the PSMA block. These conditions ensured a high propagation rate for the SMA comonomers, while limiting the homopolymerization of styrene monomers (Sty-Sty defects). Following this method, a high conversion (>82 %) for each block was achieved (Table S7), and the final material was obtained with a theoretical molar mass comparable to previous materials, and relatively good control over molar mass distribution (Table 1 – Figure S38-S40). Similarly to the diblock copolymer, the presence of two distinct peaks in the ^{13}C NMR spectrum confirmed the presence of blocks with different nature (SSS *vs.* MSM) (Figure 1 - B).

Synthesis of multisite (PSty-*s*-MAnh)$_4$-PSty

The synthesis and characterization of the multisite PSMA are detailed in our previous paper.[40] This original architecture was prepared in order to obtain a well-defined graft copolymer with low density and precise anchoring location of the side chains. The synthesis of the multisite copolymer was designed accordingly in order to distribute at least one MAnh unit (1.5 eq. used) on every 10 units of Sty, on average. The final copolymer was composed of 5 PSty blocks of DP = 10 each connected with 6 MAnh units on average, as 1.5 eq. of MAnh was added for each single monomer unit insertion (SMUI) step. The final multisite copolymer exhibited relatively narrow dispersity and molar mass comparable to previous materials (Table 1). The ^{13}C NMR spectrum showed a major peak corresponding to homopolystyrene (144-148 ppm) and minor peaks corresponding to random and alternating sequences (Figure 1 – A). This was in good agreement with the expected structure as few MAnh units were dispersed locally in the PSty backbone, either as single monomer units (random triad) or as short alternating blocks (alternating and random triads).

Synthesis of graft PSMA copolymers

All PSMA materials were functionalized by reacting the MAnh units with behenyl alcohol (C22) yielding graft-PSMA analogues (Scheme 1). Long alkyl chains were selected as functional side groups enabling graft-PSMA materials for use as potential rheology modifiers in the oil industry.[59-61] The full esterification of MAnh moieties was achieved in the presence of methane sulfonic acid under reflux of toluene in a Dean-Stark apparatus following a similar process used for 4xCTA preparation. The esterification yield, average number of alkyl chains grafted, and molar mass of the final materials were determined by IR, quantitative ^{1}H and ^{13}C NMR spectroscopy and triple-detection SEC (3d-SEC) (Supporting Information - Functionalization sections). The IR spectrum showed a complete disappearance of the MAnh carbonyl symmetric and asymmetric stretch peaks at 1,850 cm^{-1} and 1,770 cm^{-1}, respectively, and appearance of an ester carbonyl stretching peak at 1,730 cm^{-1}. Additionally, the introduction of long alkyl chains greatly increased the intensity of the alkane C-H stretch peaks at 2,700-3,000 cm^{-1}. The number of alkyl chains grafted onto each backbone was determined from the ^{13}C NMR spectrum using the C_{arom} of Sty as the reference peak (δ_c = 126 ppm) and the peak from the methylene group adjacent to an ester linkage (64.5 ppm). Interestingly, the final number of alkyl chains inserted was consistent with the theoretical average number of MAnh inserted in the backbone, confirming the original backbone composition (Table 2). The yield of esterification was calculated by comparing the number of alkyl chains grafted to the number of maleic anhydride units in each chain, determined previously. High yield of esterification (> 87 %) was confirmed for all materials. The alt-PSMA showed a slightly lower esterification yield as a result of limitations imposed by steric hindrance due to the higher MAnh density in the backbone. For this reason, the esterification of the 4xPSMA star polymer with similar MAnh density to the linear alt-PSMA was left to react longer (38 hours *vs.* 20 hours), which resulted in a higher esterification yield.

Table 2. Evolution of PSMA features after grafting

	PSMA Backbones			Graft PSMAs				
Materials	$M_{n,3d\text{-}SEC}$[a] g mol^{-1}	$Đ_{RI}$[b]	MAnh[c]	N_{graft}[d]	% Yield[e]	$M_{n,calc}$[f] g mol^{-1}	$M_{n,3d\text{-}SEC}$[a] g mol^{-1}	$Đ_{RI}$[b]
Alt-Linear	6,200 [h]	1.13 [h]	23	40	87	18,700	21,900 [g]	1.16 [g]
Diblock	6,400 [g]	1.22 [h]	13	25	96	13,800	14,700 [g]	1.12 [g]
Multiblock	5,100 [g]	1.20 [g]	10	19	95	11,200	11,100 [g]	1.17 [g]
Multisite	6,400 [g]	1.29 [g]	5	10	99	9,200	9,300 [g]	1.20 [g]
Alt-Linear	48,200 [h]	1.19 [h]	225	394	87	179,800	174,200 [g]	1.26 [g]
Alt-Star	44,900 [h]	1.15 [h]	200	396	99	177,100	180,200 [g]	1.21 [g]

[a] Obtained using triple-detection SEC (3d-SEC). [b] Obtained using conventional SEC with RI detector. [c] Number of MAnh units calculated from ^{13}C-NMR using peak at 172 ppm. [d] Calculated from ^{13}C-NMR using peak at 64.5 ppm. [e] Functionalisation yield calculated by comparing the number of alkyl chains grafted with number of MAnh units inserted. [f] Calculated from ^{13}C-NMR using $M_{n,theo}$ backbone + N_{graft} x $M_{w,Alkyl}$. [g] SEC in Chloroform. [h] SEC in DMF

Both materials with higher molar mass (linear and star 50k) showed comparable molar mass after grafting (≈ 180,000 g mol^{-1}). For all materials, a shift of the initial molar mass distribution towards higher molar mass and retention of narrow dispersity were observed after functionalization (Table 2 – SI - Functionalization sections). The true molar mass values obtained by triple-detection were shown to be in good agreement with the calculated molar masses, confirming the complete esterification of the PSMA backbones, and the synthesis of functional materials with excellent control of side chain incorporation.

Comparison of PSMA materials features and properties

The different graft architectures (linear alternating, diblock, multiblock, and multisite) were prepared from PSMA backbones with comparable molar masses, as shown by triple-detection SEC and MALDI-ToF-MS (Figure 2).

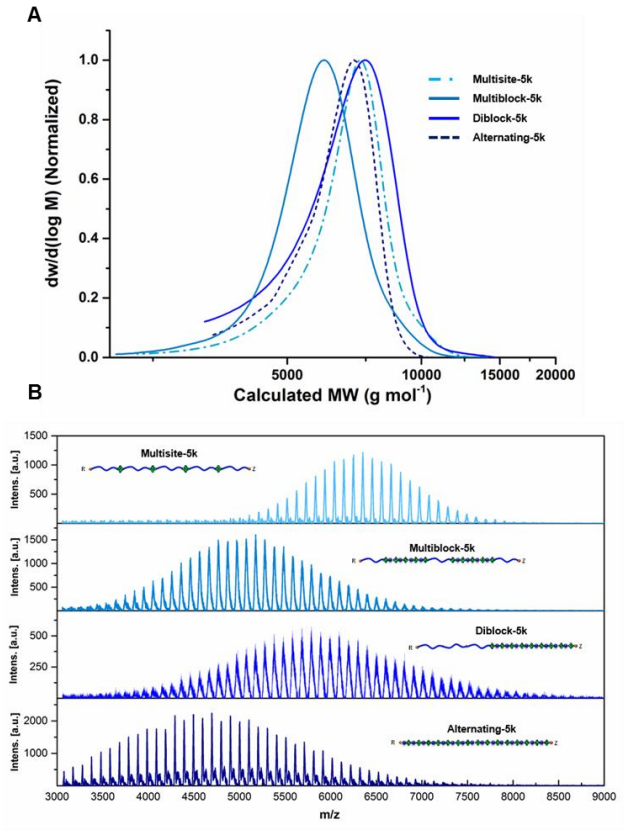

Figure 2. Comparison of molar mass distribution for short PSMA backbones measured by triple-detection SEC (A) and MALDI-ToF-MS (B).

While conventional SEC (DRI detection) provides relative information on molar mass distribution and allows good comparison of polymers of similar nature, limited information can be obtained compared to more advanced detection methods. Here, triple-detection SEC (DRI, VS, and LS) was used to determine the true molar mass ($M_{n\text{-}3d\text{-}SEC}$) and gain complementary information, such as the hydrodynamic radius (R_h) (molecular size parameter), and the intrinsic viscosity (IV) and Mark-Houwink parameter (α).

Study of materials behaviors in solution by 3d-SEC

The direct comparison of the materials behaviors in solution was limited by their solubility as they were not all soluble in the same solvent. The alt-PSMAs with high content of MAnh exhibited poor solubility in $CHCl_3$ and therefore were analyzed in DMF. On the other hand, all other grafted materials showed good solubility in $CHCl_3$. All the non-grafted linear polymers (*ca*. 6,000 g mol^{-1}) had similar R_h (1.8-1.9 nm) indicating that the MAnh density and distribution have a negligible effect on their molecular size (Table 3). Moreover, all polymers adopted random coil conformations in their respective solvents according to the Mark-Houwink parameter values ($\alpha > 0.5$).[62, 63] No significant differences were observed with respect to intrinsic viscosity, which is expected for copolymers of similar molar mass, density and conformation. As expected, an increase in molecular size was observed for longer copolymers (50,000 g mol^{-1}). The 4xPSMA was smaller in molecular size compared to the linear alt-PSMA, which is attributed to its slightly lower molar mass. Moreover, it is usually observed that star polymers adopt a more compact structural conformation compared to their linear counterparts.[62, 63] Herein, both alt-PSMA and 4xPSMA appeared to adopt similar hard sphere conformation in DMF ($\alpha < 0.5$), however, a difference in intrinsic viscosity was observed (0.356 for linear *vs.* 0.270 for star). This was not surprising as more compact architectures (star, comb or branched) have less impact on viscosity compared to a linear counterpart of similar molar mass.[62, 63]

Table 3. Features of materials in solution

	PSMA Backbones				Grafted PSMAs			
	$M_{n,3d\text{-}SEC}$ [a] g mol^{-1}	R_h [a] (nm)	IV [a] (dl/g)	α [a]	$M_{n,3d\text{-}SEC}$ [a] g mol^{-1}	R_h [a] (nm)	IV [a] (dl/g)	α [a]
Alt-Linear	6,200 [c]	1.94 [c]	0.074 [c]	0.56 [c]	21,900 [b]	2.89 [b]	0.069 [b]	0.71 [b]
Diblock	6,400 [b]	1.87 [b]	0.065 [b]	0.88 [b]	14,700 [b]	2.61 [b]	0.077 [b]	0.73 [b]
Multiblock	5,100 [b]	1.79 [b]	0.072 [b]	0.86 [b]	11,100 [b]	2.42 [b]	0.080 [b]	0.83 [b]
Multisite	6,400 [b]	1.90 [b]	0.068 [b]	0.73 [b]	9,300 [b]	2.30 [b]	0.081 [b]	0.72 [b]
Alt-Linear	48,200 [c]	6.51 [c]	0.356 [c]	0.28 [c]	174,200 [b]	8.82 [b]	0.248 [b]	0.59 [b]
Alt-Star	44,900 [c]	5.77 [c]	0.270 [c]	0.30 [c]	180,200 [b]	8.26 [b]	0.196 [b]	0.69 [b]

[a] Obtained from triple-detection SEC (RI, Viscometer, LS) using *d*n/*d*c values measured off-line. [b] SEC in Chloroform. [c] SEC in DMF

After functionalization, the molecular size was found to correlate with the grafting density and the backbone length. For the materials allowing the comparison before and after functionalization (where analysis in the same solvent was possible), slightly lower, or similar, α values were observed after grafting, due to a more compact structure. Overall, the side chain density and distribution did not impact the structures in solution as all the polymers displayed similar α values (α ≈ 0.7-0.8), corresponding to random coil conformation. For the diblock, multiblock and multisite materials, an increase in IV was observed after grafting which was expected due to the increase in molar mass. A correlation between grafting density and a decrease in IV was observed, regardless of the increase of molar mass (from 9,300 g mol^{-1} for grafted multisite to 21,900 g mol^{-1} for the alternating counterpart). This indicated that the grafting density of side chains had more impact on structure density than the molar mass. The longer graft alt-PSMA and 4xPSMA copolymers showed similar molecular size and appeared to adopt a random coil conformation while being slightly more compact compared to the short backbone materials (α ≈ 0.6-0.7). Moreover, they showed a drastic increase in IV (from 0.069 to 0.248 dl/g), expected due to the difference of molar mass. The lower IV observed for the star

material was expected as the increase of molecular size with respect to molar mass is slower for star materials compared to their linear counterparts.[62, 63]

Influence of material structure on thermal properties

The thermal stability of all PSMA materials was evaluated by thermogravimetric analysis (TGA) under N_2 gas flow in the temperature range 25-650 °C, at a heating rate of 10 °C/min. The evolution of the mass loss with temperature and the corresponding differential thermogravimetric curves (dTG) for all materials are shown in Figure 3 (details in SI – Thermal analysis sections). Three distinct degradation steps were observed, where temperature of degradation and rate of degradation depend on the material's chemical composition and structure (*i.e*. MAnh density, Mw, functionalization degree). The first step (100-200 °C), predominantly observed for the copolymers with high content of MAnh (*i.e*. alt-PSMA) is due to the release of water, CO_2, and CO from the cyclization of partially hydrolyzed MAnh and its decomposition.[64-66] The second step was attributed to the thermal degradation of the trithiocarbonate (-CS_3-) end group of CTA which usually occurs from 200-300 °C for PSty synthesized by RAFT.[67, 68] A third degradation step from 325-450 °C was observed for all the materials and is attributed to the degradation of the polymer backbone and aliphatic chains. Control analysis performed on CTA-Ester and aliphatic chains (Figure S53) confirmed a first mass loss for CTA-Ester between 200-270 °C (-CS_3- degradation), followed by a second degradation step from 270-350 °C (CTA alkyl chain degradation), which overlaps with the aliphatic chain degradation from 250-350 °C.

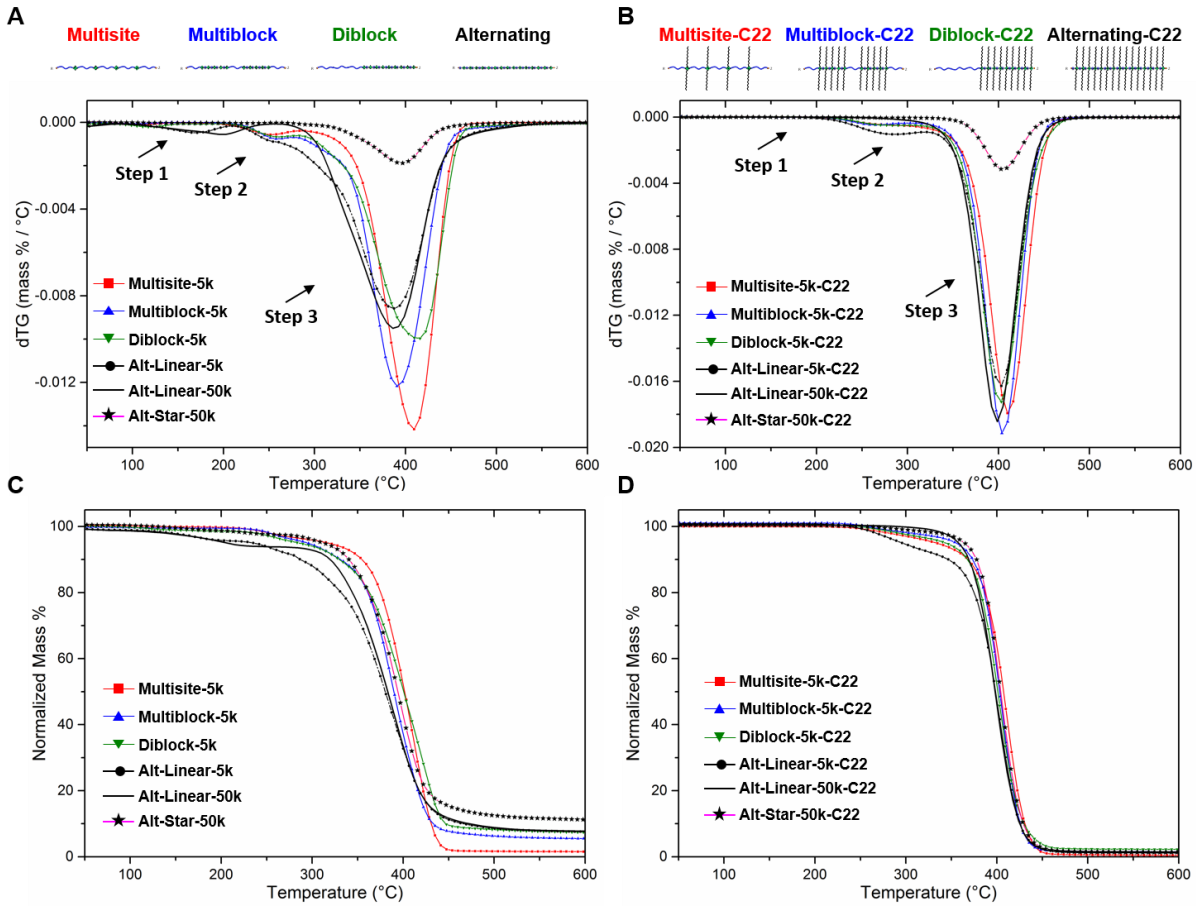

Figure 3. Derivative of mass loss (top) and mass loss (bottom) for PSMA materials before (left) and after (right) functionalization measured by TGA.

The PSMA backbones (Figure 3 - A and C) exhibited a maximum rate of degradation temperature (T_i) from 390-410 °C (Table S8). While an intermediate T_i was observed for the 4xPSMA (400 °C), the T_i for linear-PSMA and the multiblock materials were observed at a temperature 20 °C lower compared to the multisite and diblock. Moreover, a correlation between MAnh content and a decrease of the onset of degradation temperature and the rate of degradation (dTG) was observed. This confirmed the influence of material composition, monomer distribution and type of architecture on thermal stability of PSMA materials. By comparing the two linear PSMAs (5k and 50k g mol^{-1}), similar T_i and rates of degradation were observed, indicating no significant effect of the molar mass. Interestingly, the 4xPSMA was slightly more stable (onset ≈ 340 °C *vs.* 320 °C) and exhibited slower kinetics of degradation

in contrast to its linear analogue, potentially due to the increase of intermolecular interactions (cross-linking). These observations clearly showed a correlation between the macromolecular structure and thermal stability of the polymers.

After grafting with the alkyl chains (Figure 3 - B and D), all the linear PSMAs degrade with very similar profiles at higher temperature and with higher rates of degradation. No major differences were observed, indicating no influence of the grafting density and distribution on thermal stability of the alkyl functionalized materials. The star material showed also higher rate of degradation after grafting, however the degradation kinetics remained slower than linear materials, confirming the influence of the architecture (Figure 3 - B). Regarding the total mass loss, it is noteworthy that all the grafted materials were fully degraded before the temperature reached 500 °C, whereas PSMA backbones produced some residues, which appears to correlate with their MAnh content (Figure 3 – C D). The carbonization of PSMA has been reported before and is due to the transformation of cyclic and heterocyclic compounds to pyrolytic carbons at temperatures above 500 °C.[69] The higher amount of residues obtained for the 4xPSMA is due to the higher compactness, facilitating intermolecular interactions and carbonization process.

Differential scanning calorimetry (DSC) was used to investigate the influence of monomer distribution and the effect of addition of crystalline side chains on a material's glass transition and/or crystallization and melting behavior. Experimentally, three heating and cooling cycles were performed and the temperature values obtained at the second or third cycle were considered for comparison (Table S9). This is important as the first heating cycle contains the polymer's prior thermal history and is influenced by the release of water, CO_2, and CO from the cyclization and degradation of partially hydrolyzed PSMA materials at low temperature (as shown by TGA analysis). Previous studies of the thermal properties of alternating PSMA reported amorphous behavior, with T_g values between 150 °C and 202 °C depending on molar

mass.[48, 49, 70] Interestingly, the alt-PSMAs synthesized in this study covered a range of molar masses from 5,000 g mol^{-1} to 50,000 g mol^{-1} and all showed similar glass transition temperatures above 200 °C (Figure 4). The variation of T_g values reported from one study to another was previously shown to be dependent on MAnh content and potentially due to the cyclization, degradation and cross-linking occurring in the first heating cycle modifying the copolymer composition and, therefore, the T_g values measured.[64]

Previous studies on diblock and triblock (PSMA-*b*-PSty or PSMA-*b*-PSty-*b*-PSMA) showed one or two glass transition temperatures, depending on the fraction of each block.[71] For copolymers with a short PSMA block compared to PSty block, only one T_g corresponding to polystyrene was observed (100 °C) and the PSMA block was assumed miscible with PSty block.[72] Conversely, when the fraction of each block was similar, a new glass transition temperature close to pure PSMA was observed (150-200 °C).[49, 50] In the present study, the diblock copolymer was composed of two blocks of similar length and exhibited two T_g (99 °C and 168 °C) close to the values expected for each block, showing the phase separation of these blocks.

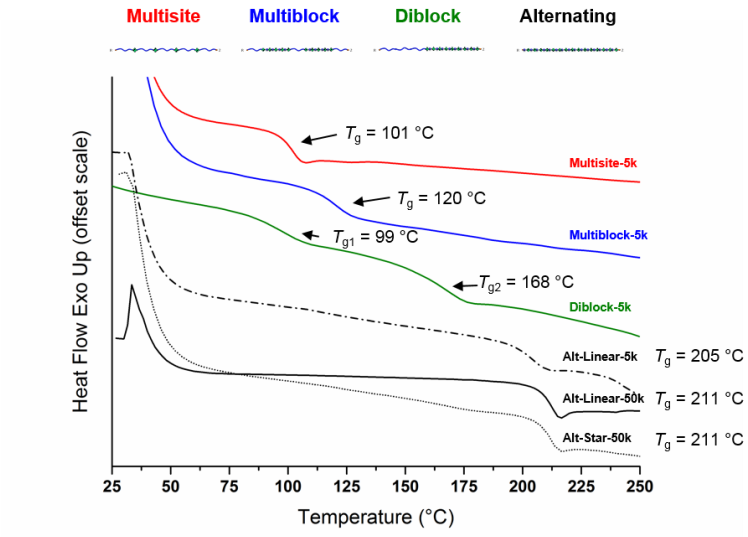

Figure 4. DSC heat flow graphs showing the third heating cycles for all PSMA backbones.

The multiblock and multisite copolymers exhibited only one T_g (120 °C and 101 °C, respectively), with the latter showing a T_g similar to polystyrene (102 °C). The multiblock showed only one T_g indicating that the SMA blocks (DP = 5) were not long enough to provide phase separation. Interestingly, the comparison of all PSMA microstructures presented in this study showed a correlation between increasing MAnh content and glass transition temperatures (Figure 4).

The grafted materials revealed completely different behavior as all the materials became semi-crystalline, regardless of the density of alkyl side chains (Figure 5 – Table S9). For the alternating materials, similar melting and crystallization temperatures were observed, showing no impact of molar mass or architecture (linear *vs.* star) on the thermal behavior, which appeared to be driven by the presence of long alkyl chains only. The crystalline behavior of copolymers with long paraffin-like side chains has already been discussed in literature.[73, 74] Moreover, the influence of copolymer microstructure on melting point was recently observed in a study on comb copolymers with long alkyl side chains.[17] The reported melting (T_m = 40-45 °C) and crystallization (T_c = 30-35 °C) temperatures were slightly lower compared to those observed in the present study for grafted alt-PSMA ($T_m \approx 53$ °C ; $T_c \approx 40$ °C). As observed previously, a lower melting temperature and a tailing were observed during the second heating cycle (DSC curves in SI). This is due to the slow reorganization of the crystalline phase which has not been completed by the end of the first cooling cycle. While alt-PSMA (high density of crystalline side chains) and diblock showed a sharp peak at similar melting temperature, broader peaks and lower melting temperatures were observed for multiblock and multisite materials, showing the poor reorganization of these materials. Interestingly, most of the materials exhibited crystallization temperatures from 30-40 °C, however, the crystallization point of the multisite copolymer dropped to 8 °C. The late crystallization and slow rearrangement of the multisite was explained by the presence of a high fraction of amorphous

polystyrene and low alkyl chain density in this material. Furthermore, the space between each alkyl chain may potentially affect their intermolecular stacking, preventing high crystallization. This observation was of great interest and demonstrates the potential of controlling the density and distribution of side chain functionalities to tune material properties.

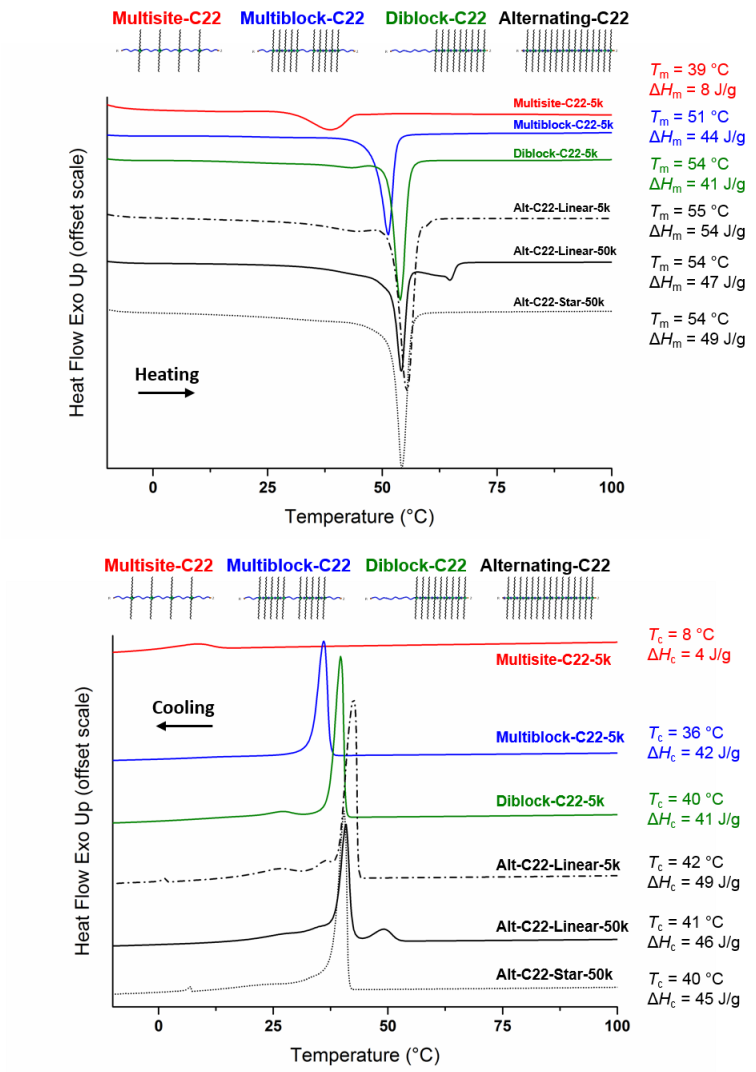

Figure 5. DSC heat flow graphs showing the second heating (top) and cooling (bottom) cycles for all functional materials

CONCLUSION

In this study we describe the synthesis of library of well-defined PSMA architectures including linear multisite, multiblock, diblock, alternating PSMA, and for the first time, an alternating 4xPSMA star. Their synthesis on gram scale was achieved by optimized RAFT polymerization using industrial RAFT agents (CTA-Acid and CTA-Ester). Furthermore, the industrial grade CTA-Ester (80 % pure) was used without purification, demonstrating the robustness of the RAFT process and anticipating large scale production. The PSMA materials were subsequently functionalized with long aliphatic alcohols, leading to graft copolymers with controlled side group density and distribution. The influence of copolymer composition and structure, and the effect of long alkyl chain addition on copolymer's behavior in solution and the thermal properties were investigated. The polymer behaviors in solution was shown to be dependent on copolymer molar mass and grafting density (increase of R_h and IV). The material degradation profiles were shown to be influenced by MAnh content, molar mass and polymeric architectures. While materials before grafting exhibited amorphous behaviors, with T_g values depending on MAnh content and distribution, a semi-crystalline behaviors was observed for all materials after adding long alkyl side chains. The alternating materials exhibited similar melting and crystallization temperatures, showing no impact of molar mass or architecture (linear *vs.* star) on the thermal behavior, which appeared to be driven by the presence of long alkyl chains only. The crystallization temperature was shown to be highly dependent on side chain density and distribution. While alt-PSMA (high density of crystalline side chains) and diblock showed a sharp peak at similar melting temperature, broader peaks and lower melting temperatures were observed for multiblock and multisite materials, showing the poor reorganization of these materials. Interestingly, all functionalized materials exhibited a crystallization temperature from 30-40 °C, however, the crystallization point of the multisite copolymer dropped to 8 °C. This study demonstrates the importance of controlling copolymer

composition and architecture for future development of material properties.

ASSOCIATED CONTENT

Supporting Information.

Experiment and characterization details including synthesis procedures, NMR spectra, SEC traces, MALDI-ToF spectra and IR spectra.

The following files are available free of charge.

AUTHOR INFORMATION

Corresponding Author

* E-mail: s.perrier@warwick.ac.uk

The authors declare no competing financial interest

ACKNOWLEDGMENT

The Authors (G.M. and S.P.) acknowledge Lubrizol for funding and for providing chemicals. We are grateful for the Polymer Characterization RTP (Daniel Lester) for providing use of the following equipment: SEC instruments, TGA and DSC. Thanks to Warwick Chemistry NMR facility (Ivan Prokes) for the advanced NMR measurements. J.T. acknowledges funding by EPSRC (EP/F500378/1).

REFERENCES

(1) Lutz, J.-F.; Ouchi, M.; Liu, D. R.; Sawamoto, M. Sequence-Controlled Polymers. *Science* **2013**, 341 (6146), 1238149.
(2) Lutz, J.-F.; Lehn, J.-M.; Meijer, E. W.; Matyjaszewski, K. From precision polymers to complex materials and systems. *Nat. Rev. Mat.* **2016**, 1 (5), 16024.
(3) Lin, T.-P.; Chang, A. B.; Chen, H.-Y.; Liberman-Martin, A. L.; Bates, C. M.; Voegtle, M. J.; Bauer, C. A.; Grubbs, R. H. Control of Grafting Density and Distribution in Graft Polymers by Living Ring-Opening Metathesis Copolymerization. *J. Am. Chem. Soc.* **2017**, 139 (10), 3896-3903.
(4) Kerr, A.; Hartlieb, M.; Sanchis, J.; Smith, T.; Perrier, S. Complex multiblock bottle-brush architectures by RAFT polymerization. *Chem. Commun.* **2017**, 53 (87), 11901-11904
(5) Polymeropoulos, G.; Zapsas, G.; Ntetsikas, K.; Bilalis, P.; Gnanou, Y.; Hadjichristidis, N. 50th Anniversary Perspective: Polymers with Complex Architectures. *Macromolecules* **2017**, 50 (4), 1253-1290.
(6) Ren, J. M.; McKenzie, T. G.; Fu, Q.; Wong, E. H. H.; Xu, J.; An, Z.; Shanmugam, S.; Davis, T. P.; Boyer, C.; Qiao, G. G. Star Polymers. *Chem. Rev.* **2016**, 116 (12), 6743-6836.
(7) Zamfir, M.; Lutz, J.-F. Ultra-precise insertion of functional monomers in chain-growth polymerizations. *Nat. Commun.* **2012**, 3, 1138.
(8) Pfeifer, S.; Lutz, J.-F. A Facile Procedure for Controlling Monomer Sequence Distribution in Radical Chain Polymerizations. *J. Am. Chem. Soc.* **2007**, 129 (31), 9542-9543.
(9) You, Y.-z.; Hong, C.-y.; Wang, W.-p.; Wang, P.-h.; Lu, W.-q.; Pan, C.-y. A Novel Strategy To Synthesize Graft Copolymers with Controlled Branch Spacing Length and Defined Grafting Sites. *Macromolecules* **2004**, 37 (19), 7140-7145.
(10) Sheiko, S. S.; Prokhorova, S. A.; Beers, K. L.; Matyjaszewski, K.; Potemkin, I. I.; Khokhlov, A. R.; Möller, M. Single Molecule Rod−Globule Phase Transition for Brush Molecules at a Flat Interface. *Macromolecules* **2001**, 34 (23), 8354-8360.
(11) Denesyuk, N. A. Bottle-brush polymers as an intermediate between star and cylindrical polymers. *Phys. Rev. E* **2003**, 68 (3), 031803.
(12) Gallyamov, M. O.; Tartsch, B.; Khokhlov, A. R.; Sheiko, S. S.; Börner, H. G.; Matyjaszewski, K.; Möller, M. Reversible Collapse of Brushlike Macromolecules in Ethanol and Water Vapours as Revealed by Real-Time Scanning Force Microscopy. *Chem. Eur. J.* **2004**, 10 (18), 4599-4605.
(13) Paturej, J.; Sheiko, S. S.; Panyukov, S.; Rubinstein, M. Molecular structure of bottlebrush polymers in melts. *Sci. Adv.* **2016**, 2 (11), 1601478.
(14) Zhang, Q.; Ran, Q.; Zhao, H.; Shu, X.; Yang, Y.; Zhou, H.; Liu, J. pH-induced conformational changes of comb-like polycarboxylate investigated by experiment and simulation. *Colloid. Polym. Sci.* **2016**, 294 (11), 1705-1715.
(15) Daniel, W. F. M.; Burdyńska, J.; Vatankhah-Varnoosfaderani, M.; Matyjaszewski, K.; Paturej, J.; Rubinstein, M.; Dobrynin, A. V.; Sheiko, S. S. Solvent-free, supersoft and superelastic bottlebrush melts and networks. *Nat. Mater.* **2015**, 15, 183.
(16) Huang, Y.; Mai, Y.; Yang, X.; Beser, U.; Liu, J.; Zhang, F.; Yan, D.; Müllen, K.; Feng, X. Temperature-Dependent Multidimensional Self-Assembly of Polyphenylene-Based "Rod–Coil" Graft Polymers. *J. Am. Chem. Soc.* **2015**, 137 (36), 11602-11605.
(17) Srichan, S.; Kayunkid, N.; Oswald, L.; Lotz, B.; Lutz, J.-F. Synthesis and Characterization of Sequence-Controlled Semicrystalline Comb Copolymers: Influence of Primary Structure on Materials Properties. *Macromolecules* **2014**, 47 (5), 1570-1577.
(18) Watson, M. D.; Wagener, K. B. Functionalized Polyethylene via Acyclic Diene Metathesis Polymerization: Effect of Precise Placement of Functional Groups. *Macromolecules* **2000**, 33 (24), 8963-8970.

(19) Shibata, M.; Matsumoto, M.; Hirai, Y.; Takenaka, M.; Sawamoto, M.; Terashima, T. Intramolecular Folding or Intermolecular Self-Assembly of Amphiphilic Random Copolymers: On-Demand Control by Pendant Design. *Macromolecules* **2018**, 51 (10), 3738–3745.
(20) Ogura, Y.; Terashima, T.; Sawamoto, M. Amphiphilic PEG-Functionalized Gradient Copolymers via Tandem Catalysis of Living Radical Polymerization and Transesterification. *Macromolecules* **2017**, 50 (3), 822-831.
(21) Zhang, J.; Deubler, R.; Hartlieb, M.; Martin, L.; Tanaka, J.; Patyukova, E.; Topham, P. D.; Schacher, F. H.; Perrier, S. Evolution of Microphase Separation with Variations of Segments of Sequence-Controlled Multiblock Copolymers. *Macromolecules* **2017**, 50 (18), 7380-7387.
(22) Yanez-Macias, R.; Kulai, I.; Ulbrich, J.; Yildirim, T.; Sungur, P.; Hoeppener, S.; Guerrero-Santos, R.; Schubert, U. S.; Destarac, M.; Guerrero-Sanchez, C.; Harrisson, S. Thermosensitive spontaneous gradient copolymers with block- and gradient-like features. *Polym. Chem.* **2017**, 8 (34), 5023-5032.
(23) Alfrey, T.; Lavin, E. The Copolymerization of Styrene and Maleic Anhydride. *J. Am. Chem. Soc.* **1945**, 67 (11), 2044-2045.
(24) Jenkins, A. D. Alternating copolymers. *Brit. Polym. J.* **1987**, 19 (1), 91-91.
(25) Trivedi, B. C.; Culbertson, B. M., Alternating Addition Copolymerizations. In *Maleic Anhydride*, Springer US: Boston, MA, **1982**.
(26) Huang, J.; Turner, S. R. Recent advances in alternating copolymers: The synthesis, modification, and applications of precision polymers. *Polymer* **2017**, 116, 572-586.
(27) Polyscope. Polyscope promotes SMA as 'versatile' polymer modifier for amorphous thermoplastics. *Add. Polym.* **2010**, 2010 (4), 2-3.
(28) Cray Valley. SMA®. http://www.crayvalley.com/products/sma-styrene
(29) Solenis. SCRIPSET™ COPOLYMER RESINS. https://solenis.com/en/industries/specialties-wood-adhesives/innovations/scripset-copolymer-resins/
(30) Matyjaszewski, K. Atom Transfer Radical Polymerization (ATRP): Current Status and Future Perspectives. *Macromolecules* **2012**, 45 (10), 4015-4039.
(31) Anastasaki, A.; Nikolaou, V.; Nurumbetov, G.; Wilson, P.; Kempe, K.; Quinn, J. F.; Davis, T. P.; Whittaker, M. R.; Haddleton, D. M. Cu(0)-Mediated Living Radical Polymerization: A Versatile Tool for Materials Synthesis. *Chem. Rev.* **2016**, 116 (3), 835-877.
(32) Ouchi, M.; Terashima, T.; Sawamoto, M. Transition Metal-Catalyzed Living Radical Polymerization: Toward Perfection in Catalysis and Precision Polymer Synthesis. *Chem. Rev.* **2009**, 109 (11), 4963-5050.
(33) Nicolas, J.; Guillaneuf, Y.; Lefay, C.; Bertin, D.; Gigmes, D.; Charleux, B. Nitroxide-mediated polymerization. *Prog. Polym. Sci.* **2013**, 38 (1), 63-235.
(34) Moad, G.; Rizzardo, E.; Thang, S. H. Living Radical Polymerization by the RAFT Process – A Third Update. *Aust. J. Chem.* **2012**, 65 (8), 985-1076.
(35) Perrier, S. 50th Anniversary Perspective: RAFT Polymerization—A User Guide. *Macromolecules* **2017**, 50 (19), 7433-7447.
(36) De Brouwer, H.; Schellekens, M. A. J.; Klumperman, B.; Monteiro, M. J.; German, A. L. Controlled radical copolymerization of styrene and maleic anhydride and the synthesis of novel polyolefin-based block copolymers by reversible addition–fragmentation chain-transfer (RAFT) polymerization. *J. Polym. Sci., Part A: Polym. Chem.* **2000**, 38 (19), 3596-3603.
(37) Park, E. S.; Kim, M. N.; Lee, I. M.; Lee, H. S.; Yoon, J. S. Living Radical Copolymerization of Styrene/MaleicAnhydride. *J. Polym. Sci., Part A: Polym. Chem.* **2000**, 38 (12), 2239-2244.

(38) Chen, G.-Q.; Wu, Z.-Q.; Wu, J.-R.; Li, Z.-C.; Li, F.-M. Synthesis of Alternating Copolymers of N-Substituted Maleimides with Styrene via Atom Transfer Radical Polymerization. *Macromolecules* **1999**, 33 (2), 232-234.
(39) Koulouri, E. G.; Kallitsis, J. K.; Hadziioannou, G. Terminal Anhydride Functionalized Polystyrene by Atom Transfer Radical Polymerization Used for the Compatibilization of Nylon 6/PS Blends. *Macromolecules* **1999**, 32 (19), 6242-6248.
(40) Moriceau, G.; Gody, G.; Hartlieb, M.; Winn, J.; Kim, H.; Mastrangelo, A.; Smith, T.; Perrier, S. Functional multisite copolymer by one-pot sequential RAFT copolymerization of styrene and maleic anhydride. *Polym. Chem.* **2017**, 8 (28), 4152-4161.
(41) Xu, J.; Fu, C.; Shanmugam, S.; Hawker, C. J.; Moad, G.; Boyer, C. Synthesis of Discrete Oligomers by Sequential PET-RAFT Single-Unit Monomer Insertion. *Angew. Chem. Int. Ed.* **2017**, 56, 1-8.
(42) Zhou, C.; Qian, S.; Zhang, A.; Xu, L.; Zhu, J.; Cheng, Z.; Kang, E.-T.; Yao, F.; Fu, G. D. A well-defined amphiphilic polymer co-network from precise control of the end-functional groups of linear RAFT polymers. *RSC Adv.* **2014**, 4 (16), 8144-8156.
(43) Henry, S. M.; Convertine, A. J.; Benoit, D. S. W.; Hoffman, A. S.; Stayton, P. S. End-Functionalized Polymers and Junction-Functionalized Diblock Copolymers Via RAFT Chain Extension with Maleimido Monomers. *Bioconjugate Chem.* **2009**, 20 (6), 1122-1128.
(44) Pfeifer, S.; Lutz, J.-F. Development of a Library of N-Substituted Maleimides for the Local Functionalization of Linear Polymer Chains. *Chem. Eur. J.* **2008**, 14 (35), 10949-10957.
(45) Feng, X.-S.; Pan, C.-Y. Synthesis of Amphiphilic Miktoarm ABC Star Copolymers by RAFT Mechanism Using Maleic Anhydride as Linking Agent. *Macromolecules* **2002**, 35 (13), 4888-4893.
(46) Fu, C.; Huang, Z.; Hawker, C. J.; Moad, G.; Xu, J.; Boyer, C. RAFT-mediated, visible light-initiated single unit monomer insertion and its application in the synthesis of sequence-defined polymers. *Polym. Chem.* **2017**, 8 (32), 4637-4643.
(47) Smith, A. A. A.; Autzen, H. E.; Laursen, T.; Wu, V.; Yen, M.; Hall, A.; Hansen, S. D.; Cheng, Y.; Xu, T. Controlling Styrene Maleic Acid Lipid Particles through RAFT. *Biomacromolecules* **2017**, 18 (11), 3706-3713.
(48) Germack, D. S.; Harrisson, S.; Brown, G. O.; Wooley, K. L. Influence of the structure of nanoscopic building blocks on the assembly of micropatterned surfaces. *J. Polym. Sci., Part A: Polym. Chem.* **2006**, 44 (17), 5218-5228.
(49) Harrisson, S.; Wooley, K. L. Shell-crosslinked nanostructures from amphiphilic AB and ABA block copolymers of styrene-alt-(maleic anhydride) and styrene: polymerization, assembly and stabilization in one pot. *Chem. Commun.* **2005**, 0 (26), 3259-3261.
(50) Zhu, M.-Q.; Wei, L.-H.; Li, M.; Jiang, L.; Du, F.-S.; Li, Z.-C.; Li, F.-M. A unique synthesis of a well-defined block copolymer having alternating segments constituted by maleic anhydride and styrene and the self-assembly aggregating behavior thereof. *Chem. Commun.* **2001**, 0 (4), 365-366.
(51) Gody, G.; Maschmeyer, T.; Zetterlund, P. B.; Perrier, S. Pushing the Limit of the RAFT Process: Multiblock Copolymers by One-Pot Rapid Multiple Chain Extensions at Full Monomer Conversion. *Macromolecules* **2014**, 47 (10), 3451-3460.
(52) Brzytwa, A. J.; Johnson, J. Scaled Production of RAFT CTA–a STAR Performer. *Polym. Prepr. (Am. Chem. Soc., Div. Polym. Chem.)* **2011**, 52 (2), 533-534.
(53) Lai, J. T.; Filla, D.; Shea, R. Functional Polymers from Novel Carboxyl-Terminated Trithiocarbonates as Highly Efficient RAFT Agents. *Macromolecules* **2002**, 35 (18), 6754-6756.
(54) Klumperman, B. Mechanistic considerations on styrene-maleic anhydride copolymerization reactions. *Polym. Chem.* **2010**, 1 (5), 558-562.

(55) Gregory, A.; Stenzel, M. H. Complex polymer architectures via RAFT polymerization: From fundamental process to extending the scope using click chemistry and nature's building blocks. *Prog. Polym. Sci.* **2012**, 37 (1), 38-105.
(56) Chaffey-Millar, H.; Stenzel, M. H.; Davis, T. P.; Coote, M. L.; Barner-Kowollik, C. Design Criteria for Star Polymer Formation Processes via Living Free Radical Polymerization. *Macromolecules* **2006**, 39 (19), 6406-6419.
(57) Yao, Z.; Zhang, J.-S.; Chen, M.-L.; Li, B.-J.; Lu, Y.-Y.; Cao, K. Preparation of well-defined block copolymer having one polystyrene segment and another poly(styrene-alt-maleic anhydride) segment with RAFT polymerization. *J. Appl. Polym. Sci.* **2011**, 121 (3), 1740-1746.
(58) Chernikova, E.; Terpugova, P.; Bui, C.; Charleux, B. Effect of comonomer composition on the controlled free-radical copolymerization of styrene and maleic anhydride by reversible addition–fragmentation chain transfer (RAFT). *Polymer* **2003**, 44 (15), 4101-4107.
(59) Wu, Y.; Ni, G.; Yang, F.; Li, C.; Dong, G. Modified Maleic Anhydride Co-polymers as Pour-Point Depressants and Their Effects on Waxy Crude Oil Rheology. *Energy Fuels* **2012**, 26 (2), 995-1001.
(60) Soni, H. P.; Kiranbala; Agrawal, K. S.; Nagar, A.; Bharambe, D. P. Designing maleic anhydride-α-olifin copolymeric combs as wax crystal growth nucleators. *Fuel Process. Technol.* **2010**, 91 (9), 997-1004.
(61) Al-Sabagh, A. M.; Noor El-Din, M. R.; Morsi, R. E.; Elsabee, M. Z. Styrene-Maleic Anhydride Copolymer Esters as Flow Improvers of Waxy Crude Oil. *J. Disp. Sci. Technol.* **2009**, 30 (3), 420-426.
(62) Agilent, *A guide to multi-detector gel permeation chromatography.* **2012**, 5990-7196EN, 1-24.
(63) Striegel, A. M. Multiple Detection in Size-Exclusion Chromatography of Macromolecules. *Anal. Chem.* **2005**, 77 (5), 104-113.
(64) Świtała-Żeliazkow, M. Thermal degradation of copolymers of styrene with dicarboxylic acidsI. Alternating styrene-maleic acid copolymer. *Polym. Degrad. Stab.* **2001**, 74 (3), 579-584.
(65) Martínez, F.; Uribe, E.; Olea, A. F. Copolymerization of Maleic Anhydride with Styrene and α- Olefins. Molecular and Thermal Characterization. *J. Macromol. Sci., Part A: Pure Appl. Chem.* **2005**, 42 (8), 1063-1072.
(66) Chen, P.; Huang, X.; Zhang, Q.; Xi, K.; Jia, X. Hybrid networks based on poly(styrene-co-maleic anhydride) and N-phenylaminomethyl POSS. *Polymer* **2013**, 54 (3), 1091-1097.
(67) Postma, A.; Davis, T. P.; Evans, R. A.; Li, G.; Moad, G.; O'Shea, M. S. Synthesis of Well-Defined Polystyrene with Primary Amine End Groups through the Use of Phthalimido-Functional RAFT Agents. *Macromolecules* **2006**, 39 (16), 5293-5306.
(68) Postma, A.; Davis, T. P.; Moad, G.; O'Shea, M. S. Thermolysis of RAFT-Synthesized Polymers. A Convenient Method for Trithiocarbonate Group Elimination. *Macromolecules* **2005**, 38 (13), 5371-5374.
(69) Cascaval, C. N.; Chitanu, G.; Carpov, A. On the thermal decomposition of copolymers of maleic anhydride with styrene. *Thermochim. Acta* **1996**, 275 (2), 225-233.
(70) Qiu, G. M.; Zhu, B. K.; Xu, Y. Y.; Geckeler, K. E. Synthesis of Ultrahigh Molecular Weight Poly(styrene-alt-maleic anhydride) in Supercritical Carbon Dioxide. *Macromolecules* **2006**, 39 (9), 3231-3237.
(71) Benvenuta-Tapia, J. J.; Vivaldo-Lima, E.; Tenorio-López, J. A.; de los Ángeles Vargas-Hernández, M.; Vázquez-Torres, H. Kinetic analysis of the RAFT copolymerization of styrene and maleic anhydride by differential scanning calorimetry. *Thermochim. Acta* **2018**, 667, 93-101.

(72) Zhan, X.; He, R.; Zhang, Q.; Chen, F. Microstructure and mechanical properties of amphiphilic tetrablock copolymer elastomers via RAFT miniemulsion polymerization: influence of poly[styrene-alt-(maleic anhydride)] segments. *RSC Adv.* **2014**, 4 (93), 51201-51207.
(73) Qin, S.; Matyjaszewski, K.; Xu, H.; Sheiko, S. S. Synthesis and Visualization of Densely Grafted Molecular Brushes with Crystallizable Poly(octadecyl methacrylate) Block Segments. *Macromolecules* **2003**, 36 (3), 605-612.
(74) Plate, N. A., Shibaev, V. P., Petrukhin, B. S., Zubov, Y. A., Kargin, V. A. Structure of crystalline polymers with unbranched long side chains. *J. Polym. Sci. A1* **1971**, 9 (8), 2291-2298.